C.N.R.S.
Centre National de la Recherche Scientifique

I.N.F.N.
Instituto Nazionale di Fisica Nucleare

Back-scattering by the optical benches: results from Virgo and constraints for AdV

E. Tournefier

VIR-NOT-070A-08

Issue 1
Date: 5th September 2008

VIRGO * A joint CNRS-INFN Project
Project office: Traversa H di via Macerata - I-56021 S. Stefano a Macerata, Cascina (PI)
Secretariat: Telephone (39) 50 752 521 – Fax (39) 50 752 550 – e-mail virgo@pisa.infn.it

Contents

1 Introduction 2

2 Definitions 2

3 End benches 4
- 3.1 Coupling factor 4
- 3.2 Analysis of measurements with Virgo 5
- 3.3 Constraints for Advanced Virgo 6

4 Detection benches 7
- 4.1 AC readout and Virgo 7
  - 4.1.1 Coupling factors 7
  - 4.1.2 Analysis of measurements with Virgo 8
- 4.2 DC readout and Advanced Virgo 10
  - 4.2.1 Coupling factors 10
  - 4.2.2 Constraints for Advanced Virgo 11

5 Injection bench 11
- 5.1 Coupling factor 11
- 5.2 Analysis of measurements with Virgo 12
- 5.3 Constraints for Advanced Virgo 13

6 Summary 13

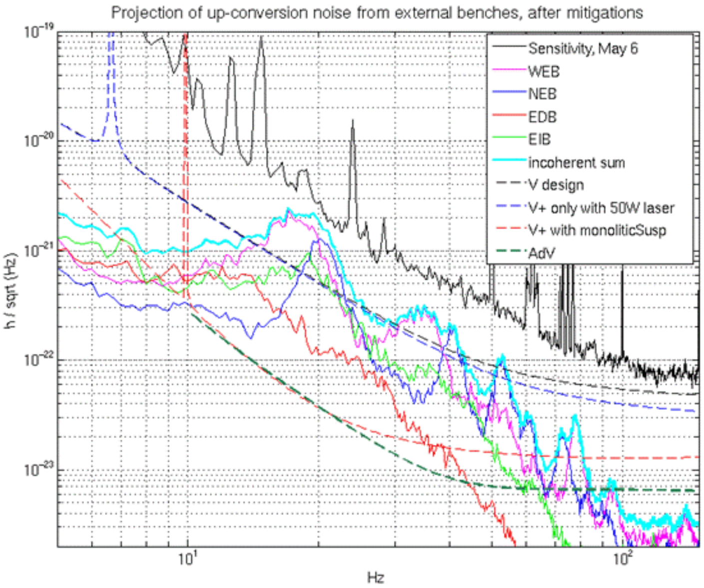

Figure 1: *Projection of diffused light noise from the optical benches on the Virgo sensitivity curve (May 2008). This Figure is extracted from [2].*

1 Introduction

After the first Virgo science run (VSR1, from May to September 2008) it was found that phase noise due to light back-scattered by the optical benches was one of the limitations to the sensitivity at low frequency. Investigations showed that the end benches, the injection external bench and the detection external bench were sources of back-scattered light and several improvements have been performed [1]. The coupling factors from the benches motion to the sensitivity was also measured [2]. These measurements also allowed to perform a noise projection showing that the noise from back-scattered light is now close to the design sensitivity [2]: Figure 1 shows the contribution of diffused light to the Virgo sensitivity curve in May 2008.
The optical coupling of this phase noise to the sensitivity can be estimated from the interferometer optical parameters and from the characteristics of the beam and the optics on these benches. In this note these coupling factors are estimated and compared to the measurements done during the Virgo commissioning. These are also estimated for Advanced Virgo in order to obtain constraints on the quantities entering in the back-scattering noise like the benches motion and the fraction of back-scattered light.

2 Definitions

A fraction f_{sc} of the beam incident on the optical benches is back-scattered by the optics and recombines with the main beam. For mirrors, photodiodes or beam dumps, f_{sc} is given by:

$$f_{sc} = \frac{P_{sc}}{P_{in}} = BRDF \frac{\lambda^2}{\pi {\omega_0}^2} \tag{1}$$

where the BRDF (Bidirectional Reflectance Distribution Function) is assumed here to be uniform and therefore defined by the average back-scatter per unit angle, and $\frac{\lambda^2}{\pi {\omega_0}^2}$ is the opening angle of the incident beam on the optic considered. BRDF have been measured at 45 degrees for typical optical components used on the Virgo benches [1]. These measurements are summarized in Table 1 and are used in the following. It is known [10] that for mirrors the BRDF function varies with $1/\theta^2$ for $\theta < \theta_1$ and is constant for $\theta > \theta_1$ with $\theta_1 \simeq 5$ degrees. Since in the following we consider some mirrors at small angle (around 10 degrees) while the measurements of BRDF were performed at 45 degrees the back-scattering might be underestimated.
For lenses the back-reflection usually dominates the back-scattering and:

$$f_{sc} = R_{AR} C_{00} \tag{2}$$

where R_{AR} is the reflectivity of the anti-reflecting coating and C_{00} is the fraction of the reflected beam which recombines to the main beam. C_{00} depends on the radius of curvature of each face of the lens and on the alignment of the lens with respect to the incident beam.
The field back-scattered or back-reflected by the optic has an amplitude proportionnal to $\sqrt{f_{sc}}$ and carries a phase noise given by:

$$\phi_{sc}(t) = \frac{4\pi}{\lambda}(x_0 + \delta x_{opt}(t)) = \phi_0 + \delta\phi_{sc}(t) \tag{3}$$

where δx_{opt} is the displacement of the optic which back-scatters the light and x_0 is a static optical path which gives the static phase ϕ_0. Typical horizontal displacements of optical benches are shown on Figure 2.
The coupling of this phase noise to the gravitational wave signal depends on the location of the scattering inside the interferometer. This coupling factor K is defined throughout this note by:

$$h_{sc} = K\sqrt{f_{sc}} \times \sin\phi_{sc} = K\sqrt{f_{sc}} \times \cos\phi_0 \times \sin\delta\phi_{sc} \tag{4}$$

where the constant term has been eliminated. Since the static phase ϕ_0 is unknown the worst case is assumed with $\phi_0 = 0$. With this assumption the coupling deduced from the measurements should be smaller than the theoritical coupling which is computed in the following. Note also that a slowly varying ϕ_0 (due to temperature effects for example) gives rise to variations of the effective coupling which is observed as non stationarities in the sensitivity.

In the following only the low to intermediate frequency (few 100 Hz) region is considered since it gives the more stringent constraint. In this region the Advanced Virgo sensitivity is modeled by:

$$h_{AdV} = 3 \times 10^{-22} \left(\frac{10}{f}\right)^3 \qquad (f < 40\text{Hz})$$

	Integrated scattering
CVI HR mirror	1400 ppm
Fichou HR mirror	200-400 ppm
Fichou Beam Splitter (R=50%)	120-170 ppm
Superpolished mirror (GO)	15-45 ppm
Lenses	15-200 ppm
Glass baffle beam dump	15-30 ppm
Standard Virgo photodiodes	2000 ppm
Quadrant Virgo photodiodes	500-800 ppm
Razor blade beam dump	~10000 ppm

Table 1: *Values of integrated scattering measured with optics used in Virgo. These values are exctracted from [1] and are the extrapolation from a measurement at 45 degrees assuming a flat BRDF (BRDF=Integrated scattering/2π).*

$$h_{AdV} = 6 \times 10^{-24} \qquad (f > 40\text{Hz}) \tag{5}$$

3 End benches

In this section the expected coupling K_{end} for light scattered by the end benches is computed. This coupling is compared to the experimental measurements in order to derive the amount of back-scattered light on these benches and check if it is coherent with the expectations. Constraints for Advanced Virgo are then derived.

3.1 Coupling factor

The power of the field back-scattered by the end benches which recouples to the main beam is given by (see also [3]):

$$P_{sc} = P_{FP} T_{end} f_{sc} T_{end} \frac{2F}{\pi} \tag{6}$$

where P_{FP} is the power stored in the Fabry-Perot cavity, T_{end} is the cavity end mirror transmission, F is the finesse of the cavity and f_{sc} is defined in Section 2. The amplitude of the back-scattered field is therefore given by:

$$A_{sc} = A_{FP} T_{end} \sqrt{\frac{2F}{\pi}} \sqrt{f_{sc}} \tag{7}$$

The total field inside the Fabry-Perot cavity is given by $A_{tot} = A_{FP} + A_{sc}$ and the phase noise induced by A_{sc} on the total field is therefore:

$$\delta\Phi = \frac{A_{sc}}{A_{FP}} \sin\phi_{sc} = T_{end} \sqrt{\frac{2F}{\pi}} \sqrt{f_{sc}} \times \sin\phi_{sc} \tag{8}$$

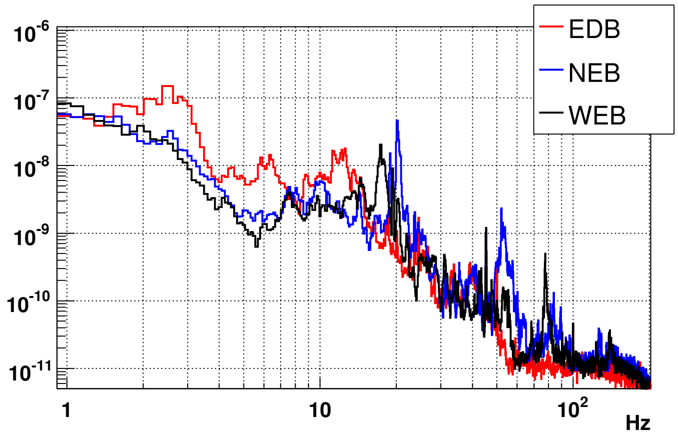

Figure 2: *Typical horizontal displacement of the Virgo optical benches in m/sqrtHz reconstructed from episensors located on the benches: external detection bench in red, north end bench in blue and west end bench in black.*

	T_{end}	F	K_{end}
Virgo	40 ppm	50	20×10^{-17}
Virgo+MS	10 ppm	150	2.9×10^{-17}
AdV low F	5 ppm	400	0.9×10^{-17}
AdV high F	5 ppm	800	0.6×10^{-17}

Table 2: *Values of the coupling factors for the light back scattered by the end benches for Virgo, Virgo+ and Advanced Virgo for given values of the end mirror transmission and of the Fabry-Perot cavity finesse.*

The gravitational wave signal equivalent to this phase noise is given by

$$h_{sc} = \frac{\lambda}{8FL}\delta\Phi \tag{9}$$

leading to a coupling factor as defined in Section 2:

$$K_{end} = \frac{\lambda}{4L}\frac{T_{end}}{\sqrt{2F\pi}} \tag{10}$$

Table 2 gives the values of these coupling factors for Virgo, Virgo+ with monolithic suspensions and Advanced Virgo.

3.2 Analysis of measurements with Virgo

The measurements performed during the commissioning of Virgo [2] gave for the north and west end benches: $K_{NE}\sqrt{f_{sc}} = 1.4 \times 10^{-20}$ and $K_{WE}\sqrt{f_{sc}} = 2 \times 10^{-20}$. From the coupling factor given in Table 2 the fraction of back-scattered light, f_{sc}, can be deduced:

$f_{sc,NE} = 0.5 \times 10^{-8}$ and $f_{sc,WE} = 1 \times 10^{-8}$.
In order to check if these values make sense the expected fraction of back-scattered light, f_{sc} should be estimated. Scattered light investigations showed that one of the most critical elements on the end benches are located inside the large telescope at the entry of the bench. The waist of the beam inside the telescope is $w_0 = 23$ μm and a measurement of BRDF for a mirror similar to those used inside the telescope gave BRDF = 100 ppm/2π [1] (as pointed out in Section 2 this could be underestimated due to the small angle of incidence on those mirrors). From Eq.1 one expects $f_{sc,tel} \simeq 1 \times 10^{-8}$ for each mirror. The photodiodes are also known to be a large source of scattered light (BRDF = 2000 ppm/2π [1]), nevertheless the backscattered light should recombine less than inside the telescope because the waist of the beam is much larger ($w_0 = 200 \mu m$): $f_{sc,phot} \simeq 2 \times 10^{-9}$.
The amount of back-scattered light deduced from the measurement of the coupling is in good agreement with what is expected from the BRDF measurements and the beam geometry on the benches: $f_{sc} \simeq 1 \times 10^{-8}$ and computations show that it is dominated by the mirrors inside the telescope. The contribution from lenses has not been estimated and could also give a non negligible contribution if these are not enough misaligned.

3.3 Constraints for Advanced Virgo

As shown with Table 2, thanks to a smaller transmission of the end mirrors and an increased finesse, the coupling factor will be reduced by a factor 7 and at least 20 for Virgo+MS and AdV respectively. The design sensitivities of Virgo+MS and AdV are about a factor 10 better than the Virgo design (Figure 1). For AdV it should therefore be possible to reduce the contribution of back-scattered light down to the design sensitivity taking advantage of the reduction of the coupling factor and with some improvements of the optical benches and/or of the environmental noise. The target will be more difficult to reach for Virgo+MS.
For AdV, using Eq.5, the coupling factor from Table 2 and a margin of a factor 10 the constraint on the product of scattered light and of the bench displacement is:

$$\sqrt{f_{sc}}\delta x_{opt} < 2.5 \times 10^{-13} \left(\frac{10}{f}\right)^3 \mathrm{m}\sqrt{W/Hz} \quad (f < 40\mathrm{Hz}) \tag{11}$$

Assuming the fraction of back-scattered light remains the same ($f_{sc,tel} \simeq 10^{-8}$) this turns into:

$$\delta x_{opt} < 2.5 \times 10^{-9} \left(\frac{10}{f}\right)^3 \mathrm{m}/\sqrt{\mathrm{Hz}} \tag{12}$$

which should be possible to acheive with in-air benches well isolated from external noises and free from resonances at low frequency [4]: see Figure 2 for the present benches displacements. The back-scattered light could also be reduced with a longer telescope (i.e a larger beam waist).

	$1-C$	K_{det}
Before OMC	3×10^{-4}	1×10^{-14}
After OMC	$< 10^{-5}$	$< 0.2\times 10^{-14}$
B5	-	1×10^{-14}

Table 3: *Values of the coupling factors for the light back scattered by the detection benches for Virgo.*

4 Detection benches

The case of the dark fringe (before or after the output mode cleaner: B1, B1p and B1s) and of the Beam Splitter pick-off beam (B5) are treated here. The AC and DC readout are treated separately since the coupling is different.

4.1 AC readout and Virgo

4.1.1 Coupling factors

One can assume that all the power (P_{sc}) back-scattered by the detection benches is reflected by the ITF towards the detection. It's amplitude should therefore be compared to the amplitude of the field stored inside the recycling cavity and similarly to Eq. 8 the phase noise induced on the total field is given by:

$$\delta\Phi = \frac{A_{sc}}{A_{rec}}\sin\phi_{sc} = \sqrt{\frac{P_{sc}}{P_{BS}}}\sin\phi_{sc} = \sqrt{\frac{f_{sc}P_{beam}}{P_{BS}}}\sin\phi_{sc} \tag{13}$$

where P_{beam} is the power of the considered beam and P_{BS} the power incident on the Beam Splitter.
In the case of the dark fringe P_{beam}=P_{df}=$P_{BS}\times(1-C)/2$. The equivalent noise in h is then given by Eq. 9 and the coupling factor is:

$$K_{det,df} = \frac{\lambda}{8FL}\sqrt{\frac{P_{df}}{P_{BS}}} = \frac{\lambda}{8FL}\sqrt{\frac{1-C}{2}} \tag{14}$$

where the contrast defect $(1-C)$ is taken before or after the output mode cleaner depending on the optic which is considered. Table 3 gives the values of this coupling factor for Virgo.

In the case of the beam reflected by the second face of the Beam Splitter (B5), P_{beam}=P_{B5}= $P_{BS}/2\times R_{BS,AR}$ where $R_{BS,AR}$ is the BS second face reflectivity ($R_{BS,AR}=4\times 10^{-4}$ in Virgo). The coupling factor is then given by:

$$K_{det,B5} = \frac{\lambda}{8FL}\sqrt{\frac{P_{B5}}{P_{BS}}} = \frac{\lambda}{8FL}\sqrt{\frac{R_{BS,AR}}{2}} \tag{15}$$

4.1.2 Analysis of measurements with Virgo

For the dark fringe, the fraction of light back-scattered (f_{sc}) by the photodiodes or the mirrors as given by Eq. 1 is attenuated or enhanced for the following reasons:

- B1 path after OMC: a Faraday isolator (isolation greater than 30dB) is placed after the OMC f_{sc} should therefore be multiplied by this attenuation factor
- B1 inside OMC: the light back-scattered inside the OMC is enhanced by $(F_{OMC}/\pi)^2$ [5]
- B1p path: this beam is only a small fraction of the dark fringe ($T_{B1p} \simeq 0.5\%$), f_{sc} should therefore be multiplied by T_{B1p}^2 (the beam goes twice through this beam splitter)
- B1s path: the beam back-scattered by B1s optics will impinge on the output mode cleaner which will only reflect higher order modes towards the ITF. These HO will then recombine to the main beam TEM_{00} inside the ITF with a coupling factor which is unknown. Only an upper limit is therefore given here setting this coupling factor to 1.
- B5: the beam back-scattered by B5 optics is attenuated by the transmission of the optics to the photodiodes and BS second face reflectivity $R_{BS,AR}$. The optics transmission should be counted twice like for B1p.

On the external detection bench the main source of scattering are the photodiodes for B1p, B5 and B1, and the HR beam splitter for B1s (B1s beam is dumped on a low scattering glass baffle). The quadrant photodiodes should not give high scattering since the power is much smaller there (and the beam size is similar). On the suspended bench the main sources of scattering are expected to be the telescope mirrors and the OMC due to the small waist. The lenses also have to be considered in the case these are well aligned with respect to the incident beam. Table 4 gives the fraction of back-scattered light for each of these components taking into account the attenuation/enhancement factors discussed above. There is more back-scattering by the optics placed on the suspended bench (OB telescope or OMC) because the waist is smaller there but since this bench moves less than the external bench the induced phase noise is not necessarily higher. The case of each bench is discussed in the following.

External detection bench

The measurements performed during the commissioning of Virgo [2] gave for the external detection bench: $K_{det} \times \sqrt{f_{sc}} < 7 \times 10^{-21}$. This is consistent with the values given in Table 4 for the elements placed on this bench (B5, B1p and B1 photodiodes and B1s beam splitter). This measurement also allows to deduce an upper limit on the attenuation factor for B1s: $f_{att,B1s} < 2\%$. This value should however be taken with care since it depends on the BRDF of the beam splitter used on B1s beam path which has not been characterized: BRDF=200 ppm/2π is assumed here.

	f_{att}	w_0 (μm)	BRDF or C_{00}	f_{sc}	$K_{det}\sqrt{f_{sc}}$
BS pick-off beam					
B5 photodiode	2×10^{-4}	200	2000ppm/2π	5×10^{-13}	8×10^{-21}
Dark fringe before OMC					
B1p photodiodes	2.5×10^{-5}	200	2000ppm/2π	6×10^{-14}	2.5×10^{-21}
B1s beam splitter	< 1	600	200ppm/2π	$< 3 \times 10^{-11}$	$< 5.5 \times 10^{-20}$
Telescope mirror	1	32	200ppm/2π	1×10^{-8}	1×10^{-18}
OB lenses	10^{-3} 10^{-3}	- -	1 ppm 10000 ppm	10^{-9} 10^{-5}	3×10^{-19} 3×10^{-17}
OMC input prism	1	140	200ppm/2π	5×10^{-10}	2×10^{-19}
Dark fringe after OMC					
B1 photodiodes	10^{-3}	600	2000ppm/2π	3×10^{-13}	1×10^{-21}
OMC (3 faces)	250	140	$3 \times$ 200ppm/2π	4×10^{-7}	1.2×10^{-18}

Table 4: *Values of the coupling factors for the light back-scattered by the optics located on the Virgo detection benches. f_{att} is the attenuation (or enhancement) factor. For the lenses the attenuation factor is given by the AR coating and the coupling coefficient (C_{00}) of the reflected beam to the main beam is assumed to be between 10^{-6} (L1 case) and 10^{-2} (L3 case, if well aligned). Beams before and after the OMC are considered separately since different coupling factors (K_{det}) should be used if the beam is taken before or after the OMC (see Table 3).*

Suspended detection bench

Back-scattered light by the suspended detection bench is mainly visible in the sensitivity at 158Hz at the level of $h = 10^{-22}/\sqrt{Hz}$. This resonance has been identified as a resonance of the first mirror of the telescope (M1) with a Q of about 40 [6]. In order to extract the value of $K_{det} \times \sqrt{f_{sc}}$ (from Eq.4)it is needed to know how much the bench moves at this frequency. Measurements of the local controls transfer function and noise injections through the local controls [7, 8, 9] allows to deduce that the bench displacement at 150Hz is $\delta z \simeq 2 \times 10^{-15}$ m/$\sqrt{Hz}$. The M1 displacement at that frequency is therefore $\delta z_{M1} \simeq 8 \times 10^{-14}$ m/$\sqrt{Hz}$ (for Q=40). It can then be deduced (using Eq. 4 and 3) that, for the suspended detection bench the experimental coupling is $K_{det} \times \sqrt{f_{sc}} \simeq 10^{-16}$. This value is higher than those computed for the main known sources of scattering listed in Table 4. This points to an unexpectedly high back-reflection by a lens or a quite high back-scattering by the OB telescope mirrors (as pointed out in Section 2 the BRDF could be higher than stated in Table 4 due to the small angle of incidence on these mirrors).

4.2 DC readout and Advanced Virgo

4.2.1 Coupling factors

In the case of DC readout the power of the carrier on the dark fringe is given by:

$$P_{df} = \frac{P_0 G_{rec}}{4}\left((1-C) + \frac{1}{2}\left(\frac{8F}{\lambda}(L_{off} + \delta L_{OG})\right)^2\right) \tag{16}$$

where L_{off} is the differential offset between the two arms of the ITF. The power of the sidebands is not considered here since, even if back-scattered before, it is filtered by the output mode cleaner. In the case of signal recycling there is an additional multiplicative factor ($T_{SR}/4$ if the carrier is anti-resonant) which is not considered here for simplicity since it does not change the results for back-scattering.
It can be assumed that all the power back-scattered by the optics is reflected back towards the detection by the ITF. The phase noise due to the scattered light is converted into power noise (δP_{sc})on B1:

$$\frac{\delta P_{sc}}{P_{B1}} = 2\sqrt{\frac{f_{sc} P_{df}}{P_{B1}}}\sin\phi_{sc} \tag{17}$$

where P_{B1} is the power after the output mode cleaner and P_{df} is the dark fringe power taken either before or after the output mode cleaner depending on the scattering optic which is considered. The signal induced by a gravitationnal wave is given by:

$$\frac{\delta P_{OG}}{P_{B1}} = 2\frac{\delta L_{OG}}{L_{off}} \tag{18}$$

and the noise induced on the sensitivity by the scattered light can be deduced from Eqs.18 and 17:

$$h_{sc} = \sqrt{f_{sc}}\sqrt{\frac{P_{df}}{P_{B1}}}\frac{L_{off}}{L}\sin\phi_{sc} \tag{19}$$

The coupling factor as defined in Section 2 is therefore:

$$K_{det,df} = \sqrt{\frac{P_{df}}{P_{B1}}}\frac{L_{off}}{L} \tag{20}$$

In the following one considers that the dark fringe power before the output mode cleaner (carrier) is of the same order of magnitude as the power on B1 so that $K_{det,df}$ simplifies to $\frac{L_{off}}{L}$ (this assumption will have to be checked). For an offset of 10 pm the value of the coupling factor is then $K_{det,df} = 3 \times 10^{-15}$, which is very similar to the Virgo case.

For the Beam Splitter pick-off beam the coupling factor is the same as for the AC readout. For $F = 800$ and assuming the BS second face reflectivity is reduced down to 1×10^{-4} for AdV (which allows to keep 100 mW on B5) the B5 coupling factor is $K_{det,B5} = 4 \times 10^{-16}$.

4.2.2 Constraints for Advanced Virgo

Using the parametrisation of the Advanced Virgo sensitivity (Eq. 5) and a safety margin of a factor 10 gives the following constraint (for $L_{off} = 10^{-11}$ m) for the Advanced Virgo dark fringe:

$$\sqrt{f_{sc}}\delta x_{opt} < 10^{-14}\left(\frac{10}{f}\right)^3 \mathrm{m}\sqrt{\mathrm{W/Hz}} \qquad (f < 40\mathrm{Hz})$$

$$\sqrt{f_{sc}}\delta x_{opt} < 2\times 10^{-17} \mathrm{m}\sqrt{\mathrm{W/Hz}} \qquad (f > 40\mathrm{Hz}) \tag{21}$$

which is very similar to what has been derived for Advanced LIGO [10]. This is an order of magnitude more stringent than for the end benches. This is nevertheless not so dramatic since, as discussed in section 4.1.2 in most cases the light backscattered by the external detection bench optics is attenuated (Faraday, beam splitters,...).
Let's assume that motion of the external bench is similar to the Virgo case i.e. $\delta x_{opt} \simeq 10^{-10}$ m/$\sqrt{Hz}$ at 40 Hz, the constraint from Eq.21 implies $f_{sc} < 4\times 10^{-14}$. Comparing this value to those given in the Virgo case in Table 4 shows that B1p photodiodes could remain on the external bench (slightly larger waist can be used as well as slightly increased attenuation) while B1 photodiodes should be placed under vacuum. B1s beam dump could remain on the external bench providing that the Faraday isolator is placed before the output mode cleaner. The bench resonance around 20 Hz (see Figure 2) should nevertheless be well attenuated or moved towards higher frequencies.

Concerning the suspended output bench we can assume it is excited by electronic noise through the local controls, therefore it's motion goes as $1/f^2$ and the more stringent constraint is around 40 Hz (providing there is no high Q resonances below few 100 Hz): $\delta x_{OB} \simeq 3\times 10^{-14}$ m/$\sqrt{Hz}$ which imples $f_{sc} < 4\times 10^{-7}$.

The coupling factor for the BS pick-off beam is about 10 times smaller than for the dark fringe (see Section 4.2.1) and B5 photodiodes could remain on an external bench. This however depends on the power needed on this beam (locking purposes). A smaller finesse would also lead to a larger coupling factor. It will therefore be better to install B5 photodiodes under vacuum.

5 Injection bench

5.1 Coupling factor

The light reflected by the injection benches recombines with the main input beam, through the Faraday isolator (located between the mode cleaner and the ITF), and induces a phase noise given by:

$$\delta\Phi_{in} = \sqrt{\frac{P_{sc}}{P_{in}}}\delta\phi_{sc} = \sqrt{\frac{f_{sc}P_{ref}}{P_{in}}}\delta\phi_{sc} \tag{22}$$

where P_{ref} is the power reflected by the interferometer. This phase noise is equivalent to a frequency noise $\delta\nu_{in} = f\delta\phi_{in}$ and is therefore reduced by the gain of the laser frequency stabilisation loop (G_{SSFS}). The frequency noise induced on the ITF input beam is therefore:

$$\delta\nu = \sqrt{\frac{f_{sc}P_{ref}}{P_{in}}}\frac{f}{G_{SSFS}}\delta\phi_{sc} \tag{23}$$

This frequency noise is equivalent to a differential arm length:

$$h_{sc} = \frac{\delta\nu}{\nu_{las}}CMRF \tag{24}$$

where CMRF is the common mode rejection factor which depends on the arms asymmetry. Between 10 and 100 Hz the CMRF is well approximated by [11]:

$$CMRF = \frac{f_{rec}}{f}\left(\frac{\Delta F}{F} + \frac{F}{2\pi}\Delta P \times G_{rec}\right) = \frac{f_{rec}}{f} \times A \tag{25}$$

where f_{rec} is the pole of the double cavity ($f_{rec} \simeq 10$ Hz in Virgo) and ΔF (resp. ΔP) is the finesse (resp. losses) asymmetry between the two Fabry Perot cavities. These two terms vary with time and can give a total contribution up to $A = 5\%$. The coupling factor is then given by:

$$K_{inj} = \sqrt{\frac{P_{ref}}{P_{in}}}\frac{f_{rec}}{G_{SSFS}}\nu_{las}A \tag{26}$$

In Virgo the reflected power is about half of the incident power and the frequency stabilisation gain below 100 Hz is $G_{SSFS} \simeq 4 \times 10^5 \times (30/f)^2$ [13], which gives:
$K_{inj} = 3 \times 10^{-21} \times (f/30)^2$.

5.2 Analysis of measurements with Virgo

The dominant source of diffused light on the external injection bench was found on B2 path [1]. After some improvements the measurement of the coupling [2] gave for the injection external bench: $K_{inj}\sqrt{f_{sc}} = 1.2 \times 10^{-20}$.
The ITF reflected beam (B2) is reflected by the Faraday isolator located on the suspended bench towards the external bench [12]. A small fraction (few %) is sent to B2 photodiodes while the largest fraction is sent on a high power beam dump. The largest scattering comes probably from this beam dump due to its high scattering (BRDF$\simeq 10^4/2\pi$ ppm) and the small waist of the beam there ($w_0 \simeq 200$ μm): one expects $f_{sc} \simeq 1.2 \times 10^{-8} \times T_{Far}$ where T_{Far} is the Faraday isolation factor which is assumed to be the same for diffused light path as for the direct beam path ($T_{Far} \simeq 10^{-3}$). One expects therefore $K_{inj}\sqrt{f_{sc}} \simeq 10^{-26} \times (f/30)^2$ for light back-scattered on B2 path. The measured coupling (1.2×10^{-20}, see above) is 5 orders of magnitude above this value. The noise observed on the dark fringe is therefore probably not a direct coupling of the phase noise carried by the scattered beam. Other possible paths for this noise are amplitude or jitter noise: this scattered light re-enters the interferometer without passing through the input mode cleaner so that it's

amplitude and jitter noise are not filtered (the only filtering comes from the Faraday isolator). To support this hypothesis, it should be underlined that this noise is visible in the DC channels of B1, B2 and B5 as would be amplitude or jitter noise. However, the amplitude noise hypothesis is not supported by noise projections so the jitter hypothesis is prefered.

5.3 Constraints for Advanced Virgo

As shown above, the direct coupling of phase noise due to back-scattered light from the reflected beam should be negligible thanks to the cancellation of this noise by the frequency stabilisation.
Let's assume that the scattered-light noise seen in Virgo enters as jitter noise. In that case the impact on the sensitivity should be similar for Advanced Virgo: according to [14] the coupling is proportionnal to $1-r_{PR}$ where r_{PR} is the PR mirror reflectivity (in amplitude). The scattering should therefore be reduced by a factor about 50 with respect to now. This could be acheived by placing improved high power beam dumps where the beam has a large waist (of the order of few mm): increasing the beam waist from $w_0 = 200$ μm to $w_0 = 2$ mm could already decrease the amount of scattered light by a factor 100.

6 Summary

The measurements of phase noise induced by back-scattered light on the optical benches have been compared to the expectations (see Table 5 for a summary). These agree well for the end benches and the the external detection bench showing that there is now no unexpected high source of back-scattering on these benches and that the coupling is well understood. On the contrary, the back-scattering on the detection suspended bench is higher than expected and possible suspects have been identified. The case of the injection is not fully understood: the measured coupling is clearly much higher than what would be expected for phase noise and other mechanisms such as amplitude or jitter noise should be looked at.

This reasonably good understanding of back-scattered light in Virgo allows then to set constraints for Advanced Virgo. At first view it does not seem necessary to put the end benches optics under vacuum and small 'in-air' improvements could be enough as proposed in [4]: more rigid benches avoiding resonances at low frequency (below about 50 Hz) and reduction of the noise from the air conditioning system. The same conclusion holds for the detection external bench except for B1 photodiodes which will have to be placed under vacuum. On the external injection bench, the main worry seems to dump the beam reflected by the ITF and the present situation can easily be improved.

Acknowledgements

I thank F. Bondu, J. Marque, B. Mours and J-Y. Vinet for discussions on scattered light issues and on this note.

	Measurement	Expectation	Highest scattering source
North end	1.4×10^{-20}	1.4×10^{-20}	mirrors inside telescope
West end	2.0×10^{-20}	1.4×10^{-20}	mirrors inside telescope
Detection external	7×10^{-21}	8×10^{-21}	B5 phot. / B1s beam dump
Detection suspended	1×10^{-16}	3×10^{-17} (upper limit)	lenses (?)
Injection external	1.2×10^{-20}	1×10^{-26}	B2 beam dump

Table 5: *Comparison of the coupling factors for diffused light phase noise from the optical benches (the coupling given here is defined by $K \times \sqrt{f_{sc}}$, see Section 2) measured in Virgo (first column) and expected (second column). The last column gives the expected largest source of diffused light for each bench.*

References

[1] B. Canuel, http://wwwcascina.virgo.infn.it/collmeetings/presentations/2008/2008-07/Commissioning/canuel_commissioning150708.ppt

[2] I. Fiori, http://wwwcascina.virgo.infn.it/commissioning/weekly/2008/May2008/Fiori_070508_NoiseProjectionNEWE.ppt and http://wwwcascina.virgo.infn.it/commissioning/weekly/2008/May2008/canuel_130508_2.ppt

[3] S. Braccini, http://wwwcascina.virgo.infn.it/collmeetings/presentations/2006/2006-02/DetectorMeeting/Braccini_Feb06_Bench_Diffusion.ppt

[4] I. Fiori, http://wwwcascina.virgo.infn.it/collmeetings/presentations/2008/2008-07/Commissioning/fiori_EnvNoise_15072008.ppt

[5] F.J. Raab, S.E. Whitcomb, LIGO-T920004-00-R (1992).

[6] I. Fiori, Virgo logbook entry 20740.

[7] D. Huet, Virgo logbook entries 19419 and 20468.

[8] D. Huet, J. Marque, E. Tournefier logbook entries 20143 and 20256.

[9] E. Tournefier, http://wwwcascina.virgo.infn.it/commissioning/weekly/2008/Jul2008/Tournefier_diffused_29Jul2008.ppt

[10] P. Fritschel, LIGO-T060303-00-D (2006).

[11] R. Flaminio, R. Gouaty, E. Tournefier, VIR-NOT-LAP-1390-313 (2006)

[12] Virgo injection benches layout, http://wwwcascina.virgo.infn.it/optics/layouts/VirgoLayout/VirgoLayout_3_4_2.pdf

[13] F. Bondu, HDR, *L'interféromètre Virgo: propriétés optiques, stabilisation en fréquence du laser*, Université Nice Sophia Antipolis (2008).

[14] Virgo Final design Report VIR-TRE-DIR-1000-13 (1997) S/Sy 4100